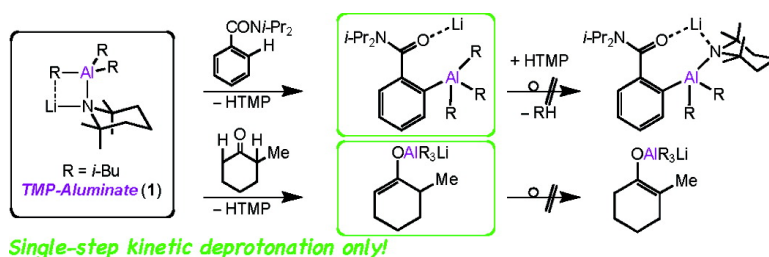


Mixed Alkylamido Aluminate as a Kinetically Controlled Base

Hiroshi Naka, James V. Morey, Joanna Haywood, Dana J. Eisler, Mary McPartlin, Felipe Garcia, Hironaga Kudo, Yoshinori Kondo, Masanobu Uchiyama, and Andrew E. H. Wheatley

J. Am. Chem. Soc., **2008**, 130 (48), 16193-16200 • DOI: 10.1021/ja804749y • Publication Date (Web): 07 November 2008

Downloaded from <http://pubs.acs.org> on February 8, 2009



More About This Article

Additional resources and features associated with this article are available within the HTML version:

- Supporting Information
- Access to high resolution figures
- Links to articles and content related to this article
- Copyright permission to reproduce figures and/or text from this article

[View the Full Text HTML](#)

Mixed Alkylamido Aluminate as a Kinetically Controlled Base

Hiroshi Naka,^{*,†} James V. Morey,[‡] Joanna Haywood,[‡] Dana J. Eisler,[‡]
Mary McPartlin,[‡] Felipe García,[‡] Hironaga Kudo,[†] Yoshinori Kondo,[†]
Masanobu Uchiyama,^{*,‡} and Andrew E. H. Wheatley^{*,‡}

Graduate School of Pharmaceutical Sciences, Tohoku University, Aobayama, Aoba-ku,
Sendai 980-8578, Japan, Department of Chemistry, University of Cambridge, Lensfield Road,
Cambridge CB2 1EW, U.K., and Advanced Elements Chemistry Laboratory, RIKEN,
2-1 Hirosawa, Wako-shi, Saitama 351-0198, Japan

Received August 16, 2007; E-mail: naka@mail.pharm.tohoku.ac.jp; uchi_yama@riken.jp; aehw2@cam.ac.uk

Abstract: The mechanisms by which directed *ortho* metalation (DoM) and postmetalation processes occur when aromatic compounds are treated with mixed alkylamido aluminate *i*-Bu₃Al(TMP)Li (TMP-aluminate **1**; TMP = 2,2,6,6-tetramethylpiperidide) have been investigated by computation and X-ray diffraction. Sequential reaction of ArC(=O)N(*i*-Pr)₂ (Ar = phenyl, 1-naphthyl) with *t*-BuLi and *i*-Bu₃Al in tetrahydrofuran affords [2-(*i*-Bu₃Al)C_mH_nC(=O)N(*i*-Pr)₂]_{Li}·3THF (*m* = 6, *n* = 4, **7**; *m* = 10, *n* = 6, **8**). These data advance the structural evidence for *ortho*-aluminated functionalized aromatics and represent model intermediates in DoM chemistry. Both **7** and **8** are found to resist reaction with HTMP, suggesting that *ortho*-aluminated aromatics are incapable of exhibiting stepwise deprotonative reactivity of the type recently shown to pertain to the related field of *ortho* zincation chemistry. Density functional theory calculations corroborate this view and reveal the existence of substantial kinetic barriers both to one-step alkyl exchange and to amido-alkyl exchange after an initial amido deprotonation reaction by aluminate bases. Rationalization of this dichotomy comes from an evaluation of the inherent Lewis acidities of the Al and Zn centers. As a representative synthetic application of this high kinetic reactivity of the TMP-aluminate, the highly regioselective deprotonative functionalization of unsymmetrical ketones both under mild conditions and at elevated temperatures is also presented.

Introduction

Organoaluminum and aluminate compounds¹ are among the most important and frequently used organometallic species in catalytic² and synthetic organic scenarios.³ Recent work has focused on their role in promoting the formation of carbon-carbon and carbon-heteroatom bonds in aliphatic systems.⁴ However, it is only recently that the potential of aromatic aluminum compounds as synthetic building blocks has begun to be developed.⁵ In particular, the generation of aluminate reagents

capable of smoothly affecting directed *ortho* metalation (DoM) chemistry⁶⁻⁹ promises to overcome limitations with the existing transmetalation methods that are employed to prepare aryl aluminum compounds, namely, the restricted compatibility of ancillary ligands (i.e., directing groups) toward aryllithium or aryl Grignard reagents.¹⁰ The resulting search for new bases capable of effecting DoM chemistry under the influence of—but without chemically altering—such directing groups led us to design the heterometallic base TMP-aluminate **1** (*i*-Bu₃Al(TMP)-Li; TMP = 2,2,6,6-tetramethylpiperidide; Chart 1) in 2004. This has subsequently been used to regio- and chemoselectively elaborate a wide variety of functionalized aromatics.¹¹

[†] Tohoku University.

[‡] University of Cambridge.

[‡] RIKEN.

- (1) (a) Mole, T.; Jeffrey, E. A. *Organoaluminum Compounds*; Elsevier: Amsterdam, 1972. (b) Negishi, E. J. *Organomet. Chem. Libr.* **1976**, *1*, 93–125.
- (2) (a) Boor, J. *Ziegler Natta Catalysts and Polymerizations*; Academic Press: New York, 1979. (b) Sasai, H.; Arai, T.; Satow, Y.; Houk, K. N.; Shibasaki, M. *J. Am. Chem. Soc.* **1995**, *117*, 6194–6198. (c) Arai, T.; Yamada, Y. M. A.; Yamamoto, N.; Sasai, H.; Shibasaki, M. *Chem. Eur. J.* **1996**, *2*, 1368–1372. (d) Arai, T.; Sasai, H.; Aoe, K.; Okamura, K.; Date, T.; Shibasaki, M. *Angew. Chem., Int. Ed. Engl.* **1996**, *35*, 104–106. (e) Arai, T.; Bougauchi, M.; Sasai, H.; Shibasaki, M. *J. Org. Chem.* **1996**, *61*, 2926–2927. (f) Iida, T.; Yamamoto, N.; Sasai, H.; Shibasaki, M. *J. Am. Chem. Soc.* **1997**, *119*, 4783–4784.
- (3) (a) Saito, S. Aluminum in Organic Synthesis. In *Main Group Metals in Organic Synthesis*; Yamamoto, H., Oshima, K., Eds.; Wiley-VCH: Weinheim, 2004; Vol. 1, Chapter 6 and references cited therein. (b) Taylor, M. S.; Zalatan, D. N.; Lerchner, A. M.; Jacobsen, E. N. *J. Am. Chem. Soc.* **2005**, *127*, 1313–1317. (c) Wieland, L. C.; Deng, H.; Snapper, M. L.; Hoveyda, A. H. *J. Am. Chem. Soc.* **2005**, *127*, 15453–15456.

- (4) (a) Novak, T.; Tan, Z.; Liang, B.; Negishi, E.-i. *J. Am. Chem. Soc.* **2005**, *127*, 2838–2839. (b) Liang, B.; Novak, T.; Tan, Z.; Negishi, E.-i. *J. Am. Chem. Soc.* **2006**, *128*, 2770–2771.
- (5) (a) Ishikawa, T.; Ogawa, A.; Hirao, T. *J. Am. Chem. Soc.* **1998**, *120*, 5124–5125. (b) Wu, K.-H.; Gau, H.-M. *J. Am. Chem. Soc.* **2006**, *128*, 14808–14809. (c) Chen, C.-A.; Wu, K.-H.; Gau, H.-M. *Angew. Chem., Int. Ed.* **2007**, *46*, 5373–5376.
- (6) For reviews on DoM see: (a) Snieckus, V. *Chem. Rev.* **1990**, *90*, 879–933. (b) Beak, P.; Meyers, A. I. *Acc. Chem. Res.* **1986**, *19*, 356–363. (c) Gschwend, H. W.; Rodriguez, H. R. *Org. React.* **1979**, *26*, 1–360.
- (7) (a) Clayden, J.; Davies, R. P.; Hendy, M. A.; Snaith, R.; Wheatley, A. E. H. *Angew. Chem., Int. Ed.* **2001**, *40*, 1238–1240. (b) Armstrong, D. R.; Boss, S. R.; Clayden, J.; Haigh, R.; Kirmani, B. A.; Linton, D. J.; Schooler, P.; Wheatley, A. E. H. *Angew. Chem., Int. Ed.* **2004**, *43*, 2135–2138.
- (8) Jantzi, K. L.; Guzei, I. A.; Reich, H. J. *Organometallics* **2006**, *25*, 5390–5395.
- (9) Sibi, M. P.; Snieckus, V. *J. Am. Chem. Soc.* **1983**, *48*, 1935–1937.

Chart 1

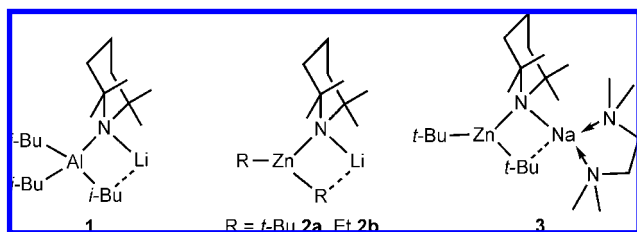
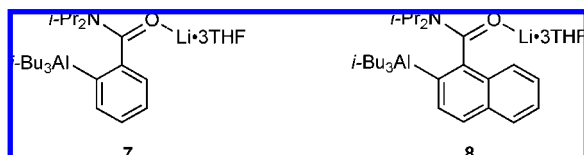


Chart 2



In the related field of organozinc chemistry, we developed TMP-zincate ($t\text{-Bu}_2\text{Zn}(\text{TMP})\text{Li}$, **2a**) as a chemoselective base in 1999,¹² its sodium analogue ($t\text{-Bu}_2\text{Zn}(\text{TMP})\text{Na}\cdot\text{TMEDA}$, **3**) having been introduced more recently by Mulvey et al.¹³ Extensive investigations of both the synthetic utility^{14–16} and structural and mechanistic properties^{17–20} of these zincates have been undertaken and have revealed that (i) deprotonation of arenes by TMP-zincates involves TMP ligand mediation rather than alkyl (e.g., $t\text{-Bu}$) ligand mediation and gives a dialkylarylzincate **4** (Scheme 1)^{17,19} and (ii) in many cases, metalated arylzincate subsequently reacts with the generated HTMP to eliminate an alkyl ligand and to give thermodynamically favorable alkylamidoarylzincate **5**.²⁰ Moreover, for $\text{DG} = \text{C}(=\text{O})\text{N}(i\text{-Pr})_2$, an alkylarylzincate has been found to form from precursor **2a** ($\text{R} = t\text{-Bu}$), while triarylzincate complex **6** has formed from **2b** ($\text{R} = \text{Et}$) by the repetition of a stepwise sequence of the type that gave **5**, demonstrating the potential for polybasicity in TMP-zincate systems.²⁰

While the polybasicity of TMP-zincates implies the possibility of systems that require only a catalytic quantity of TMP functionality, kinetically controlled bases with monobasicity are also in high

demand from a synthetic viewpoint. These would be free from undesired spectator ligand scrambling, assuring the structure and reactivity of the intermediate, and this would greatly expand their potential applications as substrates in controlled synthetic procedures. Recent structural work on aluminate chemistry has demonstrated that, in contrast to their passivity with respect to zincates, ancillary Lewis bases are susceptible to reaction with aluminate substrates.²¹ More recently, the successful isolation of *ortho* aluminate $[2\text{-}(i\text{-Bu}_3\text{Al})\text{C}_6\text{H}_4\text{C}(=\text{O})\text{N}(i\text{-Pr})_2]\text{Li}\cdot 3\text{THF}$ **7** was reported.²² However, rationalization of the observation of kinetic control (that is, amide elimination) was not attempted, and it remained unclear whether conversion of the kinetic aluminate to a thermodynamic metalate by stepwise quenching of the liberated amine was possible, *viz.*, the multifarious structure types noted for zincate chemistry.

Although zinc and aluminum are oblique neighbors in the periodic table and have been classified as typical metals with similar reactivities, their similarity is essentially superficial because they belong to different groups (Groups 12 and 13), along with the significant difference between Al(III) and Zn(II) in terms of structural and electronic properties and Lewis acidity of the central metal. Thus, it is of interest to rationalize theoretically, and corroborate experimentally, the fundamental differences between TMP-zincate and TMP-aluminate that will be of help for designing new reactions and functional ate bases containing these molecular frameworks. In this paper we report the experimental and theoretical elucidation of these metalation and postmetalation processes for TMP-aluminate **1**, focusing on its reactivity toward *N,N*-dialkylbenzamides (Scheme 2).

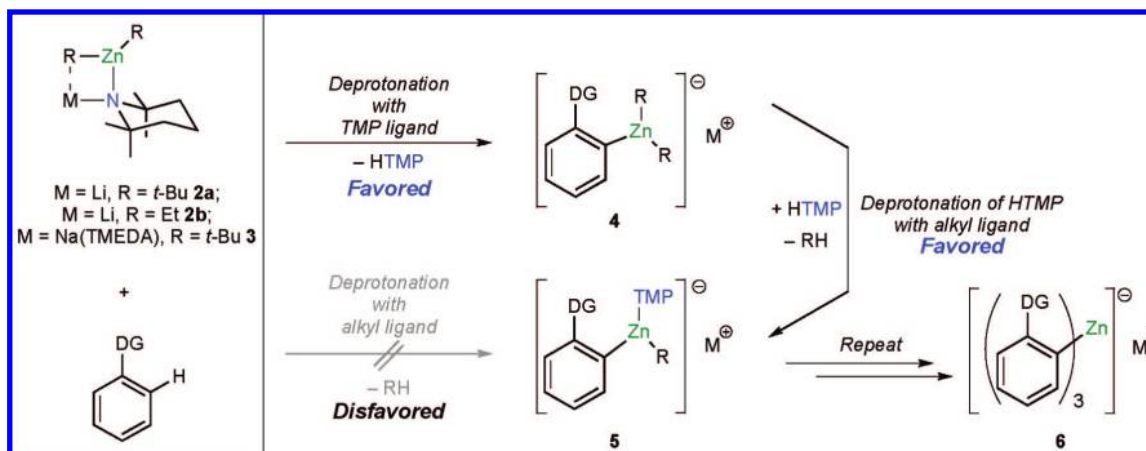
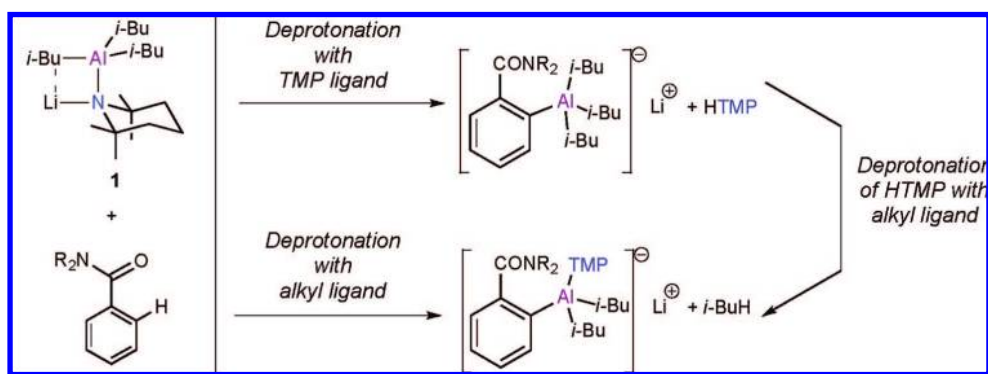
We have probed two metalation routes and one postmetalation process (as shown in Scheme 2) using density functional theory (DFT) calculations. These investigations have revealed that *ortho* alumination proceeds by a mechanism different from that exhibited by ostensibly analogous zincate bases. We next report the successful synthesis and structural characterization of *ortho*-deprotonated aromatic aluminum compounds that represent putative intermediates in directed *ortho* alumination chemistry and which have been used to examine the (in)ability of *ortho* aluminates to undergo ligand scrambling. Finally, we propose a rationalization of the demonstrable differences between TMP-aluminate and -zincate activity.

Results and Discussion

1. DFT Calculations. To shed light on the mechanism of directed *ortho* alumination, the possible pathways for the deprotonative metalation of *N,N*-dimethylbenzamide using $\text{Me}_3\text{Al}(\text{NMe}_2)\text{Li}\cdot\text{OMe}_2$ have been modeled using DFT calculations (Figure 1).²³ Although the choice of this simplified model system may lead to an underestimation of the steric effects of bulky groups (e.g., $i\text{-Bu}$), the essence of the actual reaction should still be observable in this model system.²⁴ Hence, for example, reaction of substrates **RT** gives the relatively stable electrostatic complexes **IM1** and **IM3**. In each of these, the lithium ion is associated with the carbonyl group of the aromatic

- (10) Eisch, J. J. In *Comprehensive Organometallic Chemistry*; Wilkinson, G., Stone, F. G. A., Abel, E. W., Eds.; Pergamon Press: Oxford, 1982; Vol. 6, Chap. 6 and references cited therein.
- (11) (a) Uchiyama, M.; Naka, H.; Matsumoto, Y.; Ohwada, T. *J. Am. Chem. Soc.* **2004**, *126*, 10526–10527. (b) Naka, H.; Uchiyama, M.; Matsumoto, Y.; Wheatley, A. E. H.; McPartlin, M.; Morey, J. V.; Kondo, Y. *J. Am. Chem. Soc.* **2007**, *129*, 1921–1930.
- (12) Kondo, Y.; Shilai, M.; Uchiyama, M.; Sakamoto, T. *J. Am. Chem. Soc.* **1999**, *121*, 3539–3540.
- (13) Andrikopoulos, P. C.; Armstrong, D. R.; Barley, H. R. L.; Clegg, W.; Dale, S. H.; Hevia, E.; Honeyman, G. W.; Kennedy, A. R.; Mulvey, R. E. *J. Am. Chem. Soc.* **2005**, *127*, 6184–6185.
- (14) For a review of DoM using zincate complexes, see: Mulvey, R. E.; Mongin, F.; Uchiyama, M.; Kondo, Y. *Angew. Chem., Int. Ed.* **2007**, *46*, 3802–3824.
- (15) (a) Uchiyama, M.; Miyoshi, T.; Kajihara, Y.; Sakamoto, T.; Otani, Y.; Ohwada, T.; Kondo, Y. *J. Am. Chem. Soc.* **2002**, *124*, 8514–8515. (b) Uchiyama, M.; Kobayashi, Y.; Furuyama, T.; Nakamura, S.; Kajihara, Y.; Miyoshi, T.; Sakamoto, T.; Kondo, Y.; Morokuma, K. *J. Am. Chem. Soc.* **2008**, *130*, 472–480.
- (16) Hevia, E.; Honeyman, G. W.; Kennedy, A. R.; Mulvey, R. E. *J. Am. Chem. Soc.* **2005**, *127*, 13106–13107.
- (17) Uchiyama, M.; Matsumoto, Y.; Nobuto, D.; Furuyama, T.; Yamaguchi, K.; Morokuma, K. *J. Am. Chem. Soc.* **2006**, *128*, 8748–8750.
- (18) Clegg, W.; Dale, S. H.; Harrington, R. W.; Hevia, E.; Honeyman, G. W.; Mulvey, R. E. *Angew. Chem., Int. Ed.* **2006**, *45*, 2374–2377.
- (19) Uchiyama, M.; Matsumoto, Y.; Usui, S.; Hashimoto, Y.; Morokuma, K. *Angew. Chem., Int. Ed.* **2007**, *46*, 926–929.
- (20) Kondo, Y.; Morey, J. V.; Morgan, J. C.; Naka, H.; Nobuto, D.; Raithby, P. R.; Uchiyama, M.; Wheatley, A. E. H. *J. Am. Chem. Soc.* **2007**, *129*, 12734–12738.

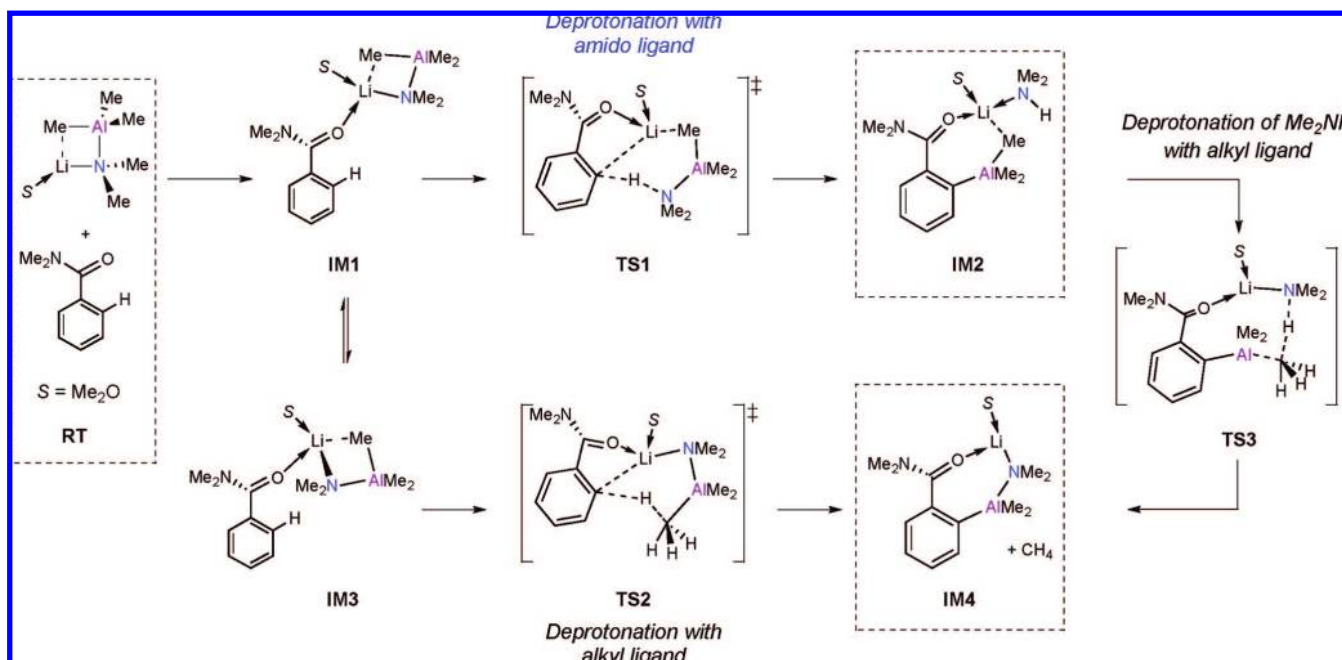
- (21) (a) García-Álvarez, J.; Graham, D. V.; Kennedy, A. R.; Mulvey, R. E.; Weatherstone, S. *Chem. Commun.* **2006**, 3208–3210. (b) García-Álvarez, J.; Hevia, E.; Kennedy, A. R.; Klett, J.; Mulvey, R. E. *Chem. Commun.* **2007**, 2402–2404.
- (22) Conway, B.; Hevia, E.; García-Álvarez, J.; Graham, D. V.; Kennedy, A. R.; Mulvey, R. E. *Chem. Commun.* **2007**, 5241–5243.
- (23) (a) Becke, A. D. *Phys. Rev. A* **1998**, *38*, 3098–3100. (b) Becke, A. D. *J. Chem. Phys.* **1993**, *98*, 1372–1377. (c) Becke, A. D. *J. Chem. Phys.* **1993**, *98*, 5648–5652. (d) Lee, C.; Yang, W.; Parr, R. G. *Phys. Rev.* **1998**, *B37*, 785–788.

Scheme 1. Stepwise DoM Pathway of TMP-Zincates (DG = Directing Group)²⁰**Scheme 2.** Possible Intermediates and Reaction Pathways in the DoM of *N,N*-Dialkylbenzamides by 1

substrate, behavior that closely resembles that observed experimentally in adducts between *N,N*-diisopropylbenzamide and R₃Al(TMP)Li (R = Me, *i*-Bu)^{11b,22} Of several possible transition states for the deprotonation of the aromatic substrate *N,N*-dimethylbenzamide, mediated by Me₂N and Me ligands on the

aluminum, we identified two (TS1 and TS2) that were accessible via reasonable activation energies (Figures 2 and 3).

The Me₂N-mediated deprotonation process (IM1-TS1-IM2) revealed an activation barrier of +30.7 kcal/mol en route to forming aluminated aromatic compound IM2. In contrast, an

**Figure 1.** Modeled pathways for the deprotonative aluminium of *N,N*-dimethylbenzamide by Me₃Al(NMe₂)Li·OMe₂: deprotonation by the NMe₂ ligand (IM1-TS1-IM2), deprotonation by a Me ligand (IM3-TS2-IM4), and quench of Me₂NH by a Me ligand (IM2-TS3-IM4).

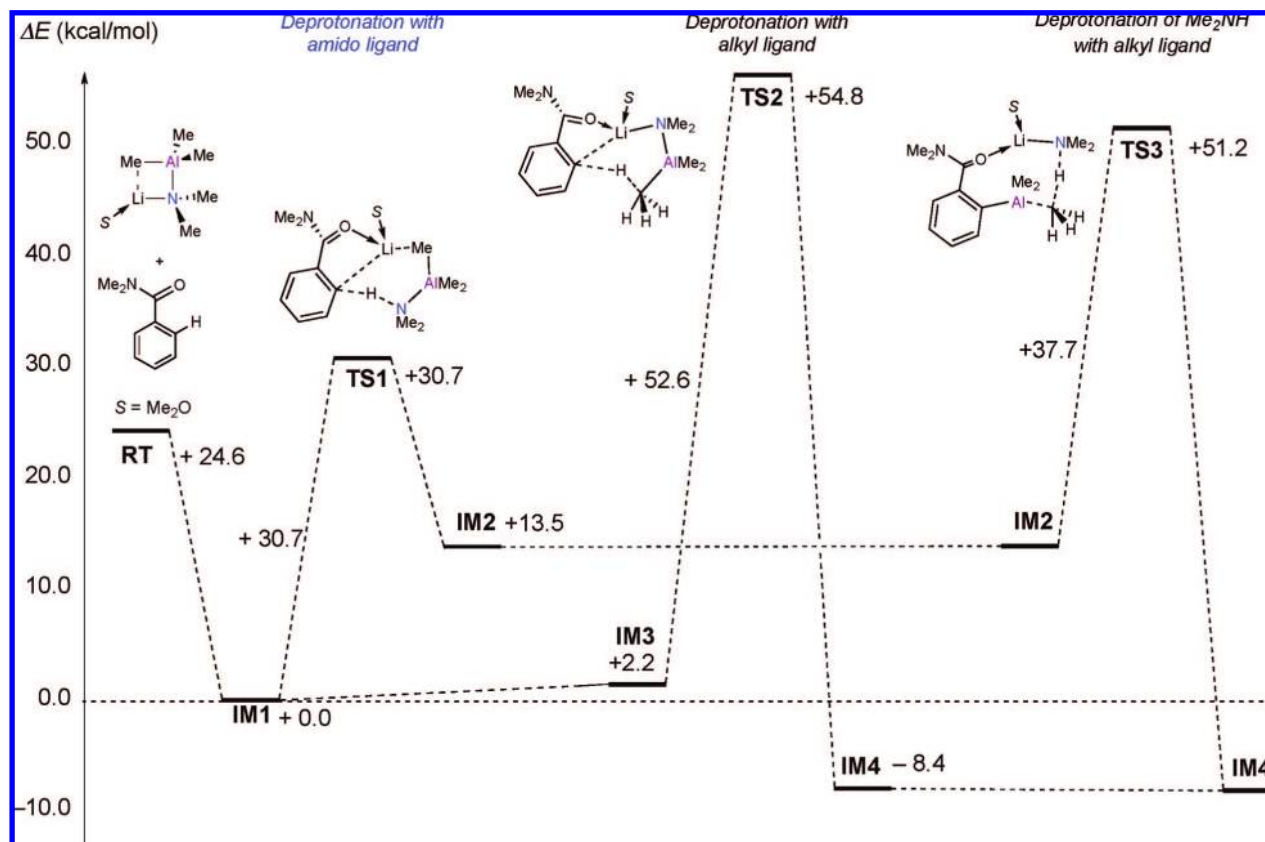


Figure 2. Summary of possible deprotonative aluminations of *N,N*-dimethylbenzamide by $\text{Me}_3\text{Al}(\text{NMe}_2)\text{Li}\cdot\text{OMe}_2$ at the B3LYP/6-31+G* level of theory. Energy changes for deprotonation by the NMe_2 ligand (TS1) with subsequent quench (TS3) or for deprotonation by the Me ligand (TS2) are shown in kcal/mol and are relative to **IM1**.²⁵

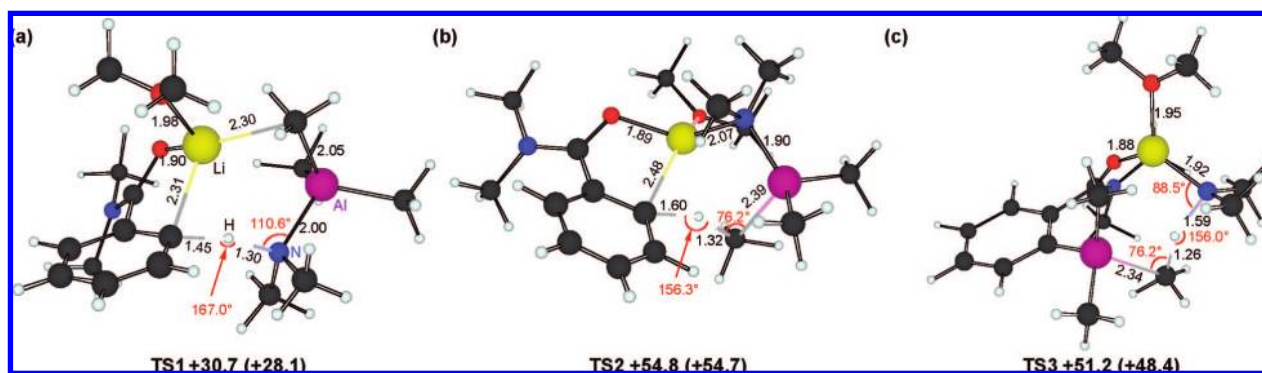


Figure 3. Transition-state structures for possible deprotonative aluminations of *N,N*-dimethylbenzamide by $\text{Me}_3\text{Al}(\text{NMe}_2)\text{Li}\cdot\text{OMe}_2$ (B3LYP/6-31+G* level): (a) deprotonation by the NMe_2 ligand (TS1); (b) deprotonation by a Me ligand (TS2); and (c) the successive quench path (TS3). Relative energies and free energies (in parentheses) are given in kcal/mol and are relative to **IM1**. TS1–3 are “open form” transition states, and no “closed form” transition states were located for these pathways.²⁶

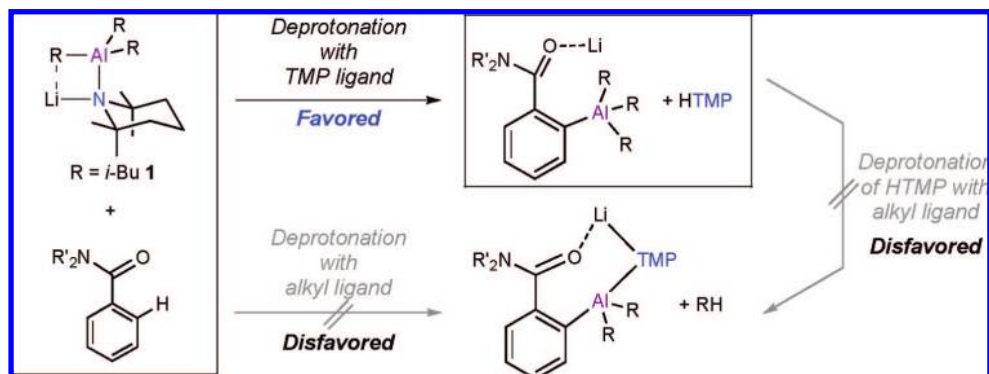
activation barrier of +52.6 kcal/mol strongly suggested that deprotonation by a methyl ligand in $\text{Me}_3\text{Al}(\text{NMe}_2)\text{Li}\cdot\text{OMe}_2$ (**IM3-TS2-IM4**) was kinetically unfavorable (TS2 being +24.1 kcal/mol less stable than TS1).^{11b} A transition state for the Me_2NH -mediated quench of a methyl ligand on the aluminum center (**IM2-TS3-IM4**) was also identified. However, this pathway required an activation barrier of +37.7 kcal/mol, and

the energy of the transition state relative to **IM1** was +51.2 kcal/mol (+20.5 kcal/mol higher than that of TS1 and only 3.6 kcal/mol lower than that of TS2). These data strongly suggest that the deprotonation of Me_2NH by an Al-bonded alkyl ligand is very unlikely—a conclusion significantly at odds with a recent tandem DFT/structural study of zincate reactivity²⁰ but consistent with crystallographic observation of trialkylaluminum 7.²² The free energy profiles for TS1–3 are depicted in Figure 3.²⁷ This result showed good agreement with the total electronic energies.

In summary, the calculated energies in the present system suggest that the model aluminate reagent serves exclusively as

(24) Both $\text{Me}_3\text{Al}(\text{TMP})\text{Li}$ and $\text{Me}_3\text{Al}(\text{TMP})\text{Li}\cdot\text{THF}$ adopt structures analogous to that of *i*- $\text{Bu}_3\text{Al}(\text{TMP})\text{Li}\cdot\text{THF}$. See ref 11b for details.
 (25) We have also identified an energetically plausible intermediate, **IM2'**, which can be formed by the dissociation of HNMe_2 from **IM2** (for **IM2'**, $\Delta E_{\text{rel}} = +6.9$ kcal/mol and $\Delta G_{\text{rel}} = -4.9$ kcal/mol, both energies being relative to **IM2**).

Scheme 3. Summary of the Theoretically Predicted Reactivity of 1



an amido base rather than as an alkyl base in DoM reactions. Interestingly, the successive quench of alkyl ligands by *in situ* formed secondary amine—demonstrated for zincate DoM²⁰—is not replicated here (Scheme 3).

2. Solid-State and Solution Structure and Reactivity. With the theoretical study suggesting that TMP-aluminates operate only as single-step, kinetically controlled bases in DoM, we decided to explore the predilection of a pre-isolated aluminated aromatic (cf. **IM2**) for undergoing postmetalation processes of the type described above. We took an indirect approach, first generating and characterizing a putative intermediate by the transmetalation of an *ortho* lithioarene using *i*-Bu₃Al and then investigating whether this species reacted with HTMP.

We selected *N,N*-diisopropylbenzamide and -naphthamide as suitable aromatic substrates since we had already established the stability of their sterically hindered amide functions toward *t*-BuLi.⁷ Accordingly, *ortho* lithiation in tetrahydrofuran (THF) was followed by the introduction of *i*-Bu₃Al.²⁸ The resulting systems could be made to deposit crystalline material that NMR spectroscopy suggested to be *ortho* deprotonated and to contain both Al and Li. Crystallographic analysis confirmed this, revealing the tris(THF)-solvated monomers [2-(*i*-Bu₃Al)-C_mH_nC(=O)N(*i*-Pr)₂Li]·3THF (*m* = 6, *n* = 4, **7**; *m* = 10, *n* = 6, **8**),²⁸ illustrated in Figure 4. In the course of this work, an independent determination of the structure of **7** was reported^{22,29} with bond lengths equal within experimental error to ours, so in this paper we will report only those observed for **8** and quote the literature values²² for **7**. Despite conformational disorder of some ligands in the structures of **7** and **8**, the gross structures are well established and demonstrate controlled *ortho* aluminatation by the insertion of *i*-Bu₃Al into a C–Li bond⁷ [C3–Al1

2.060(4), C44–Al2 2.062(5) Å for the two independent molecules in **8** (cf. 2.050(4) Å in **7**)²²] and with the Al center residing essentially in the aromatic plane. The alkali metal is supported by the amide carbonyl [O1–Li1 1.884(9), O5–Li2 1.874(8) Å in **8**, (cf. 1.860(7) Å in **7**)²²] and thereafter by three solvent molecules (Chart 2, Figure 4). Consistent with previously reported data on laterally lithiated aromatic tertiary amides,^{7b,30} tris(THF)-solvation means that that there is no interaction between Li⁺ and the site of deprotonation. This allows the directing tertiary amide group to reside nearly perpendicular to the aromatic plane³¹ in order to minimize steric interactions [C3–C2–C1–O1 98.9(6), C44–C43–C42–O5 97.7(6)° in **8**, (cf. 99.7(4)° in **7**)²²].

We next sought to investigate the dissolution of TMP-aluminate **1**, of *ortho* aluminates **7** and **8**, and also the behavior of solution *ortho* aluminate species in the presence of HTMP (see Supporting Information). The primary aims here were to reveal whether complexes such as **7** and **8** resist amine coordination and amine–alkyl ligand exchange (as theoretically suggested, Scheme 3), to evaluate whether tris(THF)-solvation of the alkali metal inhibits reaction or whether desolvation can occur, and last, to determine whether **7/8** act as intermediates in stepwise deprotonation²⁰ (cf. *ortho* zincate reactivity, Scheme 1). Cryoscopic measurements on both **7** and **8** in benzene point to partial desolvation occurring in solution, with mean observed molecular masses of 291–357 (for **7**) and 206–307 (for **8**), suggesting the loss of 0–1 THF molecules from **7** and 1–3 THF molecules from **8**.²⁸ This behavior has precedent in both experimental and theoretical aspects of directed metalation. Accordingly, trisolvated [2-(MeCH)₁₀H₆C(=O)N(*i*-Pr)₂]-

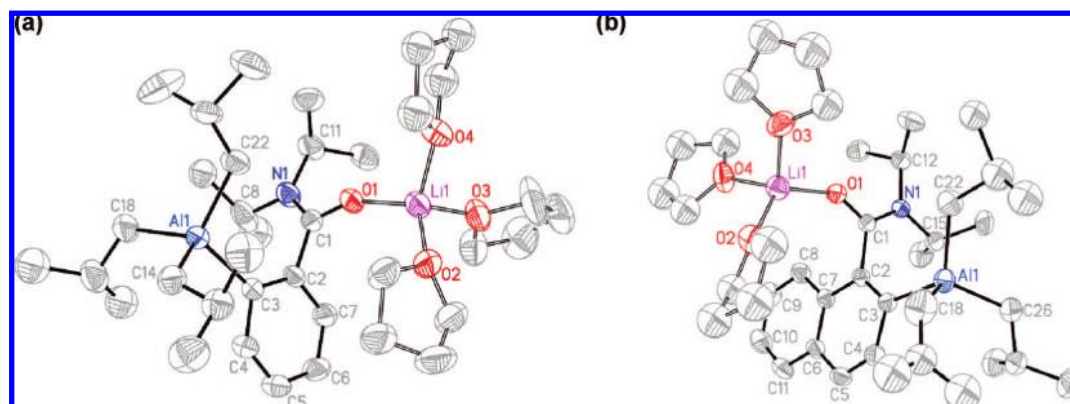


Figure 4. Molecular structures of monomeric *ortho* aluminates (a) **7** and (b) (one of the crystallographically independent molecules of) **8** plotted at 30% probability and with minor *i*-Bu and THF disorder and all H-atoms omitted for clarity. For **7** see also ref 22.

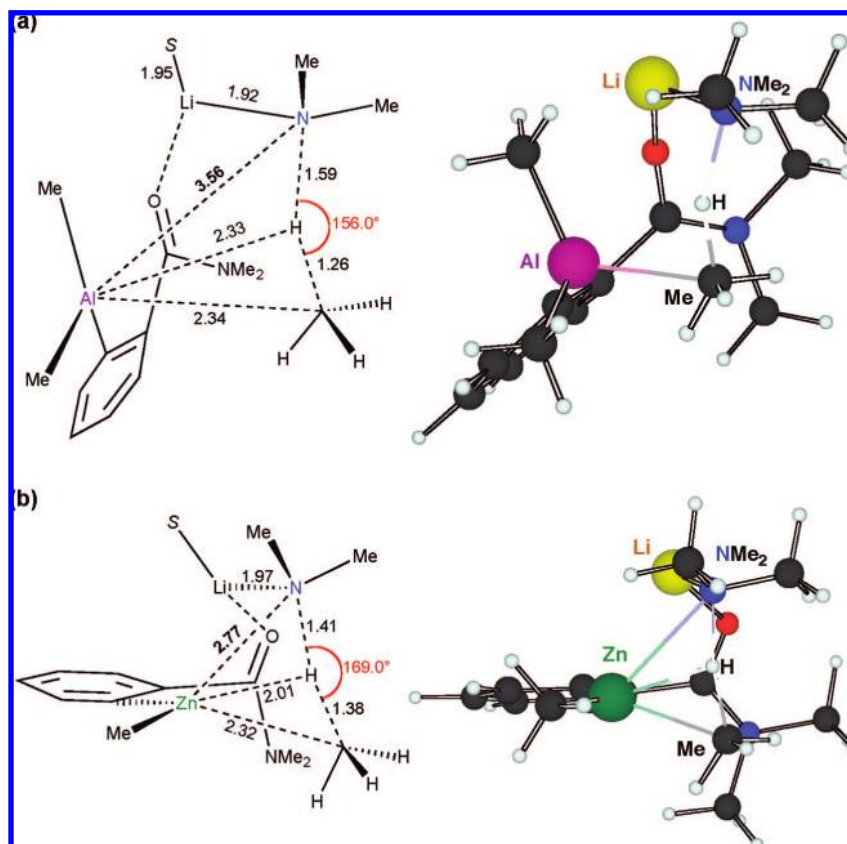


Figure 5. Optimized transition-state structures for the methyl ligand quench of secondary amine in (a) model aluminate $\text{Me}_3\text{Al}(\text{Ar})\text{Li}\cdot(\text{OMe}_2)(\text{NHMe}_2)$ (**TS3**, $\text{Ar} = \text{C}_6\text{H}_4\text{C}(=\text{O})\text{NMe}_2$, $\text{OMe}_2 = \text{S}$, B3LYP/6-31+G* level) and (b) model zincate $\text{Me}_2\text{Zn}(\text{Ar})\text{Li}\cdot(\text{OMe}_2)(\text{NHMe}_2)$ (B3LYP/631SVP level).²⁰ Solvents are omitted for clarity. Distances given in angstroms.

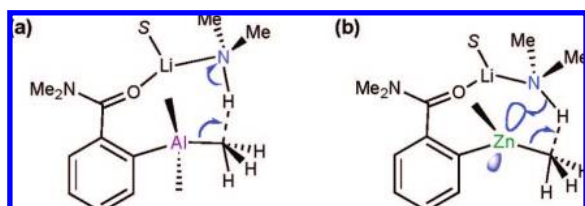


Figure 6. (a) Disfavored operation of the transition state in the deprotonation of Me_2NH by a methyl ligand bonded to Al. (b) Favored operation of the transition state in the deprotonation of Me_2NH by a methyl ligand bonded to Zn ($\text{S} = \text{OMe}_2$).

$\text{Li}\cdot 3\text{THF}$, in which the metal ion fails to interact with the deprotonated α -carbon in the lateral group in the solid state, has been shown to undergo partial desolvation with the concomitant formation of a metal–carbon bond.³⁰ Moreover, previous theoretical work has shown that, whereas *trisolvation*

of a lithiated aromatic amide electronically satisfies the metal, the removal of even one solvent molecule causes the metal to seek further coordination.^{7b} Accordingly, HTMP (1 or 2 equiv) was added to *ortho* aluminate **7** (either pre-isolated and redissolved or else generated *in situ*) in hydrocarbon solvent at room temperature. After being heated to reflux, mixtures were stored at -30°C and the crystalline deposits isolated and found to be unreacted **7** (in isolated yields of up to 69%). Evidence for the complete passivity of *ortho* aluminates toward HTMP came from ^1H and ^{13}C NMR spectroscopic analyses of samples of **7** and **8** dissolved in (nonpolar) benzene or (Lewis basic) THF before and after the introduction of excess HTMP by injection. In either solvent, chemical shifts attributable to **7** or **8** were unambiguously found to be unchanged upon the application of amine, nor was any formation of new aromatic species observed, even after heating to reflux.²⁸ The generality of this passivity has also been demonstrated by employing the aliphatic amines diethylamine and diisopropylamine in conjunction with both **7** and **8**. Finally, extensive experiments carried out on TMP-aluminate **1**, **7**, and **8** in THF (see ref 11b for **1** and Supporting Information for **7** and **8**) have established their identities in THF solution and have not shown the detectable formation of any other species, including $[\text{Li}\cdot 4\text{THF}]^+[\text{i-Bu}_4\text{Al}]^-$. While this last species was observed as a crystalline deposit by ourselves, and reported by others,²² following attempts to synthesize **1** in bulk THF, our NMR data do not

(26) (a) Zhao, P.; Collum, D. B. *J. Am. Chem. Soc.* **2003**, *125*, 4008–4009. (b) Zhao, P.; Collum, D. B. *J. Am. Chem. Soc.* **2003**, *125*, 14411–14424. (c) Zhao, P.; Condo, A.; Keresztes, I.; Collum, D. B. *J. Am. Chem. Soc.* **2004**, *126*, 3113–3118. (d) Qu, B.; Collum, D. B. *J. Am. Chem. Soc.* **2005**, *127*, 10820–10821.

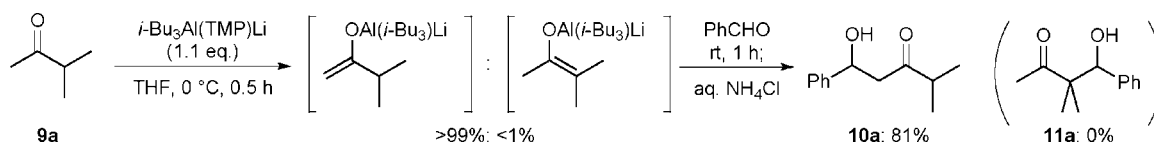
(27) The prediction of accurate Gibbs free energy profiles for reactions in solution remains a challenge for quantum chemical methods, especially in cases in which solvent exchange (association and/or dissociation) takes place at the metal atom. However, favorable error cancellation is expected in the comparison of the similar transition states **TS1–3**.

(28) See Supporting Information.

(29) The structure of **7**, reported independently, resulted from the reaction of TMP-aluminate **1** with *N,N*-diisopropylbenzamide (ref 22). Although not significantly different from ours, the reported structural parameters for **7** have slightly lower esd's.

(30) Armstrong, D. R.; Clayden, J.; Haigh, R.; Linton, D. J.; Schooler, P.; Wheatley, A. E. H. *Chem. Commun.* **2003**, 1694–1695.

(31) Bond, A.; Clayden, J.; Wheatley, A. E. H. *Acta Crystallogr. E* **2001**, *E57*, o292–o294.

Scheme 4. Regioselective Deprotonation of an Unsymmetrical Ketone Using *i*-Bu₃Al(TMP)Li (**1**)**Table 1.** Kinetically Controlled Regioselective Functionalization of Unsymmetrical Ketones Using **1**^a

entry	reactant	condition	product	yield (%)
1		0 °C, 30 min		84 ^c
2		reflux, 18 h		76 ^c
3		0 °C, 30 min		69 ^c
4		reflux, 18 h		78 ^c
5 ^d	9c	0 °C, 30 min		69

^a Unless otherwise noted, reactions were conducted using ketone (1.0 equiv) and **1** (1.1 equiv) in THF under the conditions noted, and quenched with benzaldehyde (1.0 equiv, room temperature, 1 h). ^b Isolated yield. Only a single regioisomer was detected. ^c Mixture of diastereomers. ^d Quenched with TMSCl (4.0 equiv.).

support its formation as a significant *solution* species in systems that contain, or have been treated with, **1**.

Overall, experimental evidence strongly supports the view that **7** and **8** (both putative intermediates in directed *ortho* alumination using TMP-aluminate **1**) dissolve to give a partially desolvated solution species that is, nevertheless, inert to amines. This suggests that the deprotonation of HTMP by an *i*-Bu ligand in aluminated aromatic complexes is an unlikely step in the deprotonative alumination of arenes by **1**. Consistent with the DFT analysis (*vide supra*), this conclusion contrasts markedly with that reached in our previous study of apparently analogous TMP-zincates.²⁰

3. Origin of the Differing Reactivities of TMP-Aluminates and TMP-Zincates. The present theoretical and experimental investigation has shown that TMP-aluminate **1** (i) acts as an amido base but, unlike its zincate analogues, (ii) exhibits only single-step DoM behavior. To elucidate the origin of the different reactivities observed for aluminate and zincate systems, the structures of the transition states for the quenching of amine by a metal-bonded alkyl group were analyzed in detail (Figure 5).

The structures of the transition states in Figure 5 are similar in principle: in each case the Me₂NH is deprotonated by a Me ligand in concerted (S_N2) fashion with a slightly bent N–H–Me angle (Al, 156.0°; Zn, 169.0°), the Me₂N ligand is anchored by Li⁺ (Al, N–Li 1.92 Å; Zn, N–Li 1.97 Å), and the methyl ligand is dissociating from Al or Zn to form methane (Al, Al–Me 2.34 Å; Zn, Zn–Me 2.32 Å). Importantly, however, the Me₂N⋯Al distance (3.56 Å) is significantly longer than Me₂N⋯Zn (2.77 Å), a difference that can be explained by the lower Lewis acidity of aluminum (Figure 6). Because Al is coordinatively saturated by the three alkyl moieties and the aryl ligand, it is unable to stabilize the [Me₂N][−] anion that is emerging in the transition state (Figure 6a). In contrast, zinc is unsaturated (16e in its valence shell) and is therefore capable of accepting two more electrons to achieve a saturated 18-

electron configuration (Figure 6b).³² This allows Zn to stabilize the loosely associated [Me₂N][−] anion, lowering the total activation energy for this quench step. In short, the decreased inherent Lewis acidity of Al prevents replication of the quenching process noted recently for Zn.²⁰

4. Synthetic Application of the Kinetic Basicity of TMP-Aluminate. The present DFT/solid-state/solution combined study has shown that TMP-aluminate **1** is a highly kinetically controlled base. With this kinetic reactivity, we expected that **1** should show extremely high kinetic selectivity in reactions that offer mixtures of kinetically preferred and thermodynamically preferred products. Thus, we tested the regioselective functionalization of unsymmetrical ketones using **1** (Scheme 4, Table 1).

Methyl isopropyl ketone **9a** was treated with 1.1 equiv of **1** at 0 °C in THF, and it was found that the kinetically preferred enolate was selectively formed (estimated using ¹³C NMR spectroscopy at −50 °C). Electrophilic trapping of this enolate intermediate with benzaldehyde proceeded smoothly to give only the expected regioisomer **10a** in 81% yield, with none of the thermodynamically preferred isomer **11a** being detected. Other unsymmetrical acyclic and cyclic ketones (**9b,c**) were similarly functionalized regioselectively (Table 1).

To our surprise, the regioselectivity highlighted in Table 1 was maintained even under harsh conditions, such as the reflux temperature of THF (65 °C) for 18 h (entries 2, 4). The intermediate was also trapped with TMSCl to give only the kinetic silyl enol ether **12c**. Regioselective deprotonation of these unsymmetrical ketones has hitherto required the use of lithium amides under low temperature conditions to achieve high regioselectivity and to avoid undesirable side reactions at the electrophilic functional groups.³³ In contrast, the present results clearly show that the TMP-aluminate **1** is a highly chemoselective, kinetically controlled base that can be used even at elevated temperatures.

Conclusions

In summary, the present theoretical and experimental study has revealed that TMP-aluminate **1** (i) acts as an amido base but, unlike its zincate analogues, (ii) exhibits only single-step DoM reactivity. Moreover, rationalization of this dichotomy comes from an evaluation of the inherent Lewis acidities of the Al and Zn centers.

The single-step mechanism proposed for aluminate bases points to their stoichiometric reaction. This mode of reactivity does not offer the potential, recently noted in zincate DoM chemistry,²⁰ for polybasicity and the use of a catalytic quantity of amine.³⁴ However, such stoichiometric reactivity does clarify

(32) (a) Uchiyama, M.; Koike, M.; Kameda, M.; Kondo, Y.; Sakamoto, T. *J. Am. Chem. Soc.* **1996**, *118*, 8733–8734. (b) Uchiyama, M.; Kameda, M.; Mishima, O.; Yokoyama, N.; Koike, M.; Kondo, Y.; Sakamoto, T. *J. Am. Chem. Soc.* **1998**, *120*, 4934–4946.

(33) Clayden, J. *Organolithiums: Selectivity for Synthesis*; Pergamon/Elsevier Science: Oxford, 2002.

(34) Hodgson, D. M.; Chung, Y. K.; Nuzzo, I.; Freixas, G.; Kulikiewicz, K. K.; Cleator, E.; Paris, J.-M. *J. Am. Chem. Soc.* **2007**, *129*, 4456–4462.

the status of the dummy ligand (i.e., the *i*-Bu group) and ensures freedom from undesired and uncontrolled ligand scrambling. Because the choice of spectator ligand can strongly influence the reactivity of the aromatic moiety (as a nucleophile, a base, a transmetalation reagent, a benzyne generator, etc.), such a mechanistic deduction has clear implications for future work in this field and for the design of new organometallic reagents for synthesis. Moreover, it implies that logical and controlled switching of DoM reactivity can be achieved through the selection of aluminate or zincate bases.

Acknowledgment. This research was partly supported by the Astellas Foundation, The Sumitomo Foundation, Hoansha, and a Grant-in-Aid for Young Scientists (A) from the Ministry of Education, Culture, Sports, Science and Technology, Japan (to M.U.). We also gratefully acknowledge the UK EPSRC (J.V.M., J.H., D.J.E.) and Newnham and Trinity Colleges, Cambridge (F.G.) for financial support. This research was also supported by the

Tohoku-Kaihatsu Memorial Foundation, the Exploratory Research Program for Young Scientists (ERYS), and a Grant-in-Aid for Young Scientists (B) from the Ministry of Education, Culture, Sports, Science and Technology, Japan (H.N.). We thank Prof. Paul Raithby (University of Bath, UK) for assistance with crystallography and Miss Sylvia Gonzalez-Calera for help with NMR spectroscopy. The calculations were performed using the RIKEN Super Combined Cluster (RSCC) facility. We also thank Dr. Daisuke Nobuto (The University of Tokyo) for technical assistance.

Supporting Information Available: Synthetic procedures, spectroscopic data, computational coordinates, and details of modeling programs used; X-ray crystallographic data, in CIF format. This material is available free of charge via the Internet at <http://pubs.acs.org>.

JA804749Y